

01 Sep 2019

The Potential of using Micro-Sized Crosslinked Polymer Gel to Remediate Water Leakage in Cement Sheaths

Murad Abdulfarraj

Abdulmohsin Imqam

Missouri University of Science and Technology, ahikx7@mst.edu

Follow this and additional works at: https://scholarsmine.mst.edu/geosci_geo_peteng_facwork

 Part of the [Petroleum Engineering Commons](#)

Recommended Citation

M. Abdulfarraj and A. Imqam, "The Potential of using Micro-Sized Crosslinked Polymer Gel to Remediate Water Leakage in Cement Sheaths," *Journal of Petroleum Exploration and Production Technology*, Springer Verlag, Sep 2019.

The definitive version is available at <https://doi.org/10.1007/s13202-019-00783-6>



This work is licensed under a [Creative Commons Attribution 4.0 License](#).

This Article - Journal is brought to you for free and open access by Scholars' Mine. It has been accepted for inclusion in Geosciences and Geological and Petroleum Engineering Faculty Research & Creative Works by an authorized administrator of Scholars' Mine. This work is protected by U. S. Copyright Law. Unauthorized use including reproduction for redistribution requires the permission of the copyright holder. For more information, please contact scholarsmine@mst.edu.



The potential of using micro-sized crosslinked polymer gel to remediate water leakage in cement sheaths

Murad Abdulfarraj¹ · Abdulmohsin Imqam¹

Received: 16 July 2019 / Accepted: 19 September 2019
© The Author(s) 2019

Abstract

Cementing is a major step in the construction and sealing of hydrocarbon wells. During the life cycle of the well, cement is prone to cracking due to a change in downhole conditions. This research investigates the use of micro-sized crosslinked polymer gel as a sealant material to mitigate cracked cement sheaths. Two experimental setups were designed to investigate water leakage through cement. The impact of polymer gel strength on the gel's ability to seal cement cracks was investigated using four gel strengths, including 500 pa, 1200 pa, 1450 pa, and 2440 pa. The impact of the width of the cement crack was also investigated using 0.5, 2, 3.2, and 6.75 mm. Results showed that the polymer gel propagated across fractures like a piston with no gravity effect and with angle with gravity effect. Blocking efficiency to water flow is controllable, and it can be increased if a high strength polymer gel is selected. To the authors' knowledge, very little experimental work has been conducted to investigate the use of crosslinked micro-gel in cement zonal isolation. This study can provide the oil and gas industry with a better understanding of the materials to use in improving cement zonal isolation and thus reduce the impact of cement failure.

Keywords Particle gel · Water leakage · Cement failure · Wellbore integrity

Introduction

Wellbore integrity is defined by NORSOK D-010 (2013) as the “application of technical, operational, and organizational solutions to reduce risk of uncontrolled release of formation fluids throughout the life cycle of a well.” If the cement is not properly completed and abandoned, it may develop leakages during any stage of the life of the well (Watson and Bachu 2007). Fluids (water or hydrocarbon) can migrate through pathways within the cement itself or between the cement and its surroundings. When the wellbore integrity is compromised, these pathways occur and formation fluids are allowed to migrate between formations and/or from the formation to the surface. Leakage of water, gases, and hydrocarbon fluids through cement pathways may occur during the drilling or production stage of the well, or after the abandonment of the well, which may endanger personnel and the environment (Davies et al. 2014; Alkhamis and

Imqam 2018; Ahdaya and Imqam 2019). The leakage of fluids along the interface between the wellbore and formation is a primary concern in hydrocarbon recovery (Dusseault et al. 2000). Leakage pathways in the cement annulus can happen due to mechanical failures as a result of pressure and temperature cycles, chemical degradation due to the corrosive formation fluids (Zhang and Bachu 2011; and Liu et al. 2017), or due to improper slurry design. Improper slurry design includes the use of slurries with low densities, which may allow formation fluids to create channels within the cement sheath; the use of slurries with high fluid loss, which may affect the mechanical properties of the set cement; and the use of rigid cement, which can get fracked as a result of casing expansions and contractions. Also, failures can occur due to improper mud removal. The leftover mud on the surface of the formation and casing can prevent the cement from bonding with its surroundings, creating micro-annuli. These and similar failures create pathways for formation fluids through the cement barrier.

Commonly, cement squeeze remedial operation is performed to seal cement leakages. However, cement squeeze cannot be used effectively to mitigate and prevent leakage because of low cement injectivity, pressure restriction,

✉ Abdulmohsin Imqam
ahikx7@mst.edu

¹ Missouri University of Science and Technology, Rolla, USA

pinhole leakage, micro-channels and fractures inside the leaking formation, and micro-cracks within primary cement (Jones et al. 2014). To overcome these limitations, self-healing cement was developed (Cavanagh et al. 2007; Roth et al. 2008; Reddy et al. 2010; Khatri 2013). Self-healing cement enables an automatic repair when micro-annuli, an internal cement crack, or another flow path is created. However, these kinds of sealing materials still have some problems associated with their swelling chemical additives and other concerns related to their mechanical and thermal stability. Crosslinked polyacrylamide polymer gels are another kind of sealant material that have been used in many oil field applications due to their high injectivity and ability to mitigate excessive water migration; controlling the water production increases the oil recovery (Feng et al. 2012; Deng et al. 2018; Sadati and Sahraei 2019). Polymer gel could be activated by temperature, pressure, a change in the water salinity, and a change in the pH (Vasquez and Santin 2015; Imqam et al. 2015a, b), and the strength of the gel can be increased by implementing nanomaterials (Tongwa and Baojun 2015).

Crosslinked polymer gels have also been widely known and used in the industry for conformance control, and the success of this material in enhancing hydrocarbon recovery is established (Seright 1995; Bai et al. 2007; Seright 2009; Zhang and Bai 2010; Imqam et al. 2015a, b, 2018; Yu et al. 2017). Micro-size particle gel is aggregated by water salinity. It forms at the surface and then is dried and crushed into small particles to be injected into the reservoir. No gelation occurs in the reservoir (Imqam et al. 2015a, b), though the gelation can be controlled by temperature and salinity (He et al. 2015; Zheng et al. 2017; Fuseni et al. 2018). Yet, few laboratory studies investigate its ability in cement zonal isolation. This study can provide the oil and gas industry with better understanding of the potential of using particle gel to mitigate the water leakage in cement sheaths. Thus, the ability of particle gels to plug the highly permeable zones behind casing or fractures or channels across the cement was the main motivation behind this work. The other motivation of this investigation is to test the injectivity of this material for zonal isolation application in comparing to the conventional cement materials.

This work investigates the potential of using micro-sized crosslinked polymer gel for water control to improve zonal

isolation in cement sheaths through a set of measurements that count for the injectivity and the propagation of the gel particles inside the cement cracks or fractures in addition to the effect of the fracture sizes and the importance of defining the size of the cracks in the cement to increase the possibility of successful remedial job.

Experimental description

Materials

Micro-size particle gel

A commercial super-absorbent polymer gel (polyacrylamide–acrylic acid copolymer provided by Emerging Technologies Company) was selected as the sealant material for all experiments. The material was used as it received from the emerging technologies company without any change in the chemical composition. Before swelling, the gel was a dry white granular powder.

Sodium chloride (NaCl)

A commercially available NaCl with a purity of 99.99% was used to create a brine solution.

Class H cement

All the cement specimens that were used in this study were prepared using Class H cement and distilled water. The specific gravity of the cement was found to be 3.18, using a gas pycnometer. The chemical composition of Class H cement was obtained using X-ray fluorescence spectroscopy (XRF) and is listed in Table 1.

Material preparation

Cement paste preparation

The cement slurry was mixed at room temperature using a two-speed bottom-drive blender. A specific amount of water was poured in the blender, and then dry cement was added

Table 1 Chemical composition of Class H cement

| Comp. | CaO | SiO ₂ | Fe ₂ O ₃ | Al ₂ O ₃ | SO ₃ |
|-------|-------|------------------|--------------------------------|--------------------------------|-----------------|
| wt% | 65.72 | 20.36 | 6.19 | 3.17 | 2.26 |
| Comp. | MgO | K ₂ O | SrO | TiO ₂ | Other |
| wt% | 1.32 | 0.43 | 0.21 | 0.16 | 0.18 |

at a uniform rate while mixing at low speed for around 15 s. Then, the blender was covered and the mixing continued for an extra 35 s at high speed (API RP 10B-2 2012). The cement slurry had a water/cement ratio (WCR) of 0.38 following the API specification 10A for API cement Class H (API 2010).

Fractured cement cores preparation

To prepare the fractured cement cores, one inch in diameter molds were cut into two halves (Fig. 1c). The cement was poured into each half and left for more than 72 h to set. Then, two metal sheets with specific thickness (0.5 mm and 2.0 mm) were used to separate the two cement specimens to the targeted fracture width.

Gel preparation

Initially, the gel particles were sieved using 20–40 mesh screens to obtain homogenous gel particles. Then, the brines with different concentrations were added to the gel particles and left to swell for 9–12 h. After that, the gel particles were drained for 12 h to remove excessive brine. For the gel plugging efficiency measurements, four swollen gel samples were prepared using four different NaCl concentrations (0.05, 0.25, 1, and 10%). The NaCl concentration ranges were selected based on the previous work that evaluated their impact on the swelling ratio and gel strength (Zhang and Bai 2010; Tongwa and Baojun 2015; Imqam

et al. 2015a, b, 2018). For the gel propagation analysis, two different brine concentrations (0.05 and 1%) were prepared.

Experimental methodology

Rheological measurements

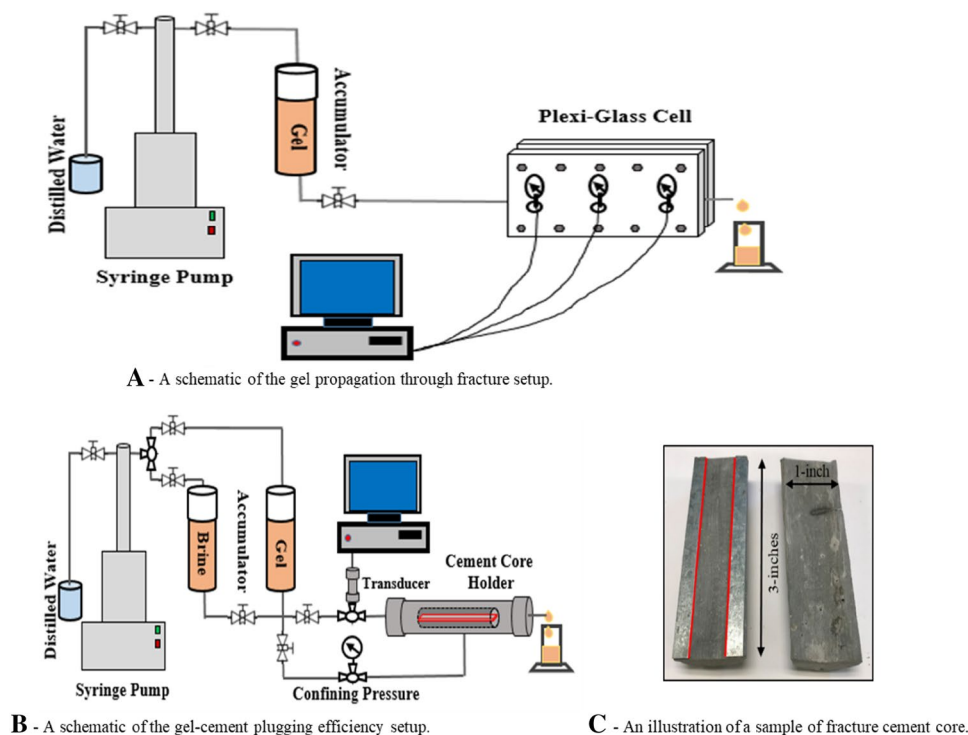
Anton Paar Modular Compact Rheometer MCR 302 Instruments with a parallel-plate system (PP50/TG using a 0.30 mm gap) were used to measure the gel strength. The measurements were taken at 25 °C to measure the gel strength of the four swollen gel samples.

Swelling gel capacity

Test tubes were used to immerse a specific amount of dry gel particles in a specific volume of brine solution. Four different brine solutions were used to determine the swelling capacity of the particle gel over time. The stable swelling ratio was computed for each concentration. The swelling ratios of the particle gel in different brine solutions were obtained using Eq. (1) (Imqam et al. 2015a, b):

$$\text{Swelling capacity} = \frac{V_2 - V_1}{V_1} \quad (1)$$

Fig. 1 An illustration of the setups used in this study and a sample of fractured cement core



where V_1 is the initial volume of the gel sample before swelling and V_2 is the final volume of the gel sample after swelling.

Experimental setups and procedures

Gel propagation through fracture

The gel propagation through the cement setup is shown in Fig. 1a. It is composed of a syringe pump, an accumulator with a piston, and an adjustable plexiglass cell. Gasket rubber was placed between the parallel plexiglass plates, which mimics the fracture width. The transparent glass cell model was used to visualize and determine the gel flow mechanisms through the fracture. Cement usually has a very low water leakage into the matrix, and therefore the fracture cell setup was designed to mimic that and to only observe the flow performance along fractures. Gel and brine were injected through the accumulator into the plexiglass cell. Pressure transducers were placed at the inlet, in the middle, and at the outlet of the cell to observe the gel performance along the fracture. Three fracture widths (0.5 mm, 3.2 mm, and 6.75 mm) were used to examine the effect of the cement fracture size on the gel injection. The fracture width sizes were selected along with gel swollen particle sizes to get different ratio ranges of gel particle size to fracture width. Table 2 gives the ratio of gel particle size to the fracture width for different gels. The ratios obtained were equal to one, below one, and above one to have a better understanding of gel passing mechanisms along different cement fracture width sizes.

Gel propagation through fracture procedure

Brine was initially injected into the plexiglass cell using an accumulator to mimic the case when the cement was already filled with water before the sealant injection. After the brine was in place, particle gel was then injected into the plexiglass cell with a constant flow rate of 1 ml/min. The gel injection continued until the gel was produced from

the outlet of the cell and the injection pressure became stable across the fracture. The injection pressure was recorded using the three pressure sensors, and a high-accuracy camera was used also to monitor the angle of gel propagation across the fracture.

Gel–cement plugging efficiency setup

The gel–cement plugging efficiency setup, as shown in Fig. 1b, is composed of a syringe pump, an accumulator with a piston, and a core holder. The pump is connected to the accumulator and is used to inject the brine and swollen gel. The cement fractured core as shown in Fig. 1c is placed in the core holder, and confining pressure is applied to prevent fluid leakage around the fractured core and to mimic the confining pressure conditions. Two fracture widths (0.5 mm and 2 mm) were used to examine the effect of cement fracture size on gel placement. A pressure transducer is used to record injection pressure.

Gel–cement plugging efficiency procedure

Gel was first injected into the fractured cement core through an accumulator with a constant flow rate of 1 ml/min. The injection stopped when the gel was produced from the core and gel injection stable pressure was achieved. After the gel was in place, brine was injected into the gel particle packed fracture to test the gel plugging efficiency to water. The brine was injected through an accumulator with a constant flow rate of 1 ml/min. The brine injection continued until the brine injection pressure became stable. The pressure data were recorded during all the experiments using transducers.

Results and analysis

The results for the rheology of the gel, the swelling capacity, gel propagation in the cement fracture, and gel plugging efficiency will be presented in this section.

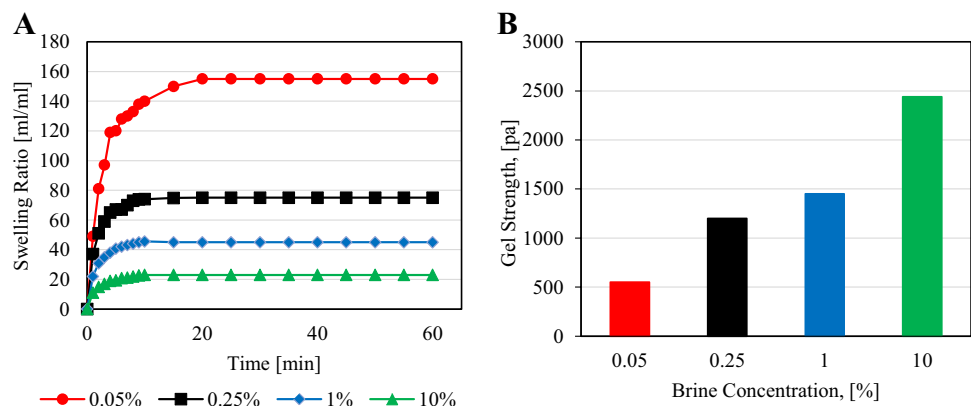
Polymer gel swelling capacity and strength results

The ability of the particle gel to absorb water is a strong function of the (NaCl) concentration (Imqam et al. 2016). As the brine concentration increases, the gel will absorb less water and its swelling will decrease. Lower gel swelling will result in a smaller particle size, but it will also result in stronger particles with higher gel strength. The change in brine concentration had a very clear effect on the swelling ratio of gel particles. The swelling ratio for the gel swollen in 0.05% NaCl reached 155 ml/ml, as shown in Fig. 2a. The swelling ratio increased from 75 to 155 ml/ml when the brine concentration decreased from 0.25% NaCl to 0.05%

Table 2 Characteristics of the polymer gel particle/opening ratio parameters

| Brine concentration [% by weight] | Swollen particle gel size [mm] | Fracture width [mm] | Gel particle size to fracture width ratio |
|-----------------------------------|--------------------------------|---------------------|---|
| 0.05 | 4.88 | 0.5 | 9.76 |
| | | 3.2 | 1.525 |
| | | 6.75 | 0.72 |
| 1 | 3.2 | 0.5 | 6.4 |
| | | 3.2 | 1 |
| | | 6.75 | 0.47 |

Fig. 2 Swelling ratio and gel strength of gel at different NaCl (by weight) concentrations



NaCl. The gel particles that swelled more became weaker and began to soften. This decrease in gel strength is most likely due to the gel absorbing a large volume of water. Figure 2b shows the measurement of the particle gel strength, which is represented by the storage modulus of the gel that was measured by the rheometer, swollen in different brine concentrations. The gel exhibited a significant increase in strength when the brine concentration increased.

Gel propagation through cement's fracture

In this section, the movement of the gel inside the cement fractures was studied by utilizing the gel propagation through a transparent cement setup (Fig. 1a). This setup was intended to study the effects of gel particle size to fracture width ratio on gel propagation performance, as described in Table 2.

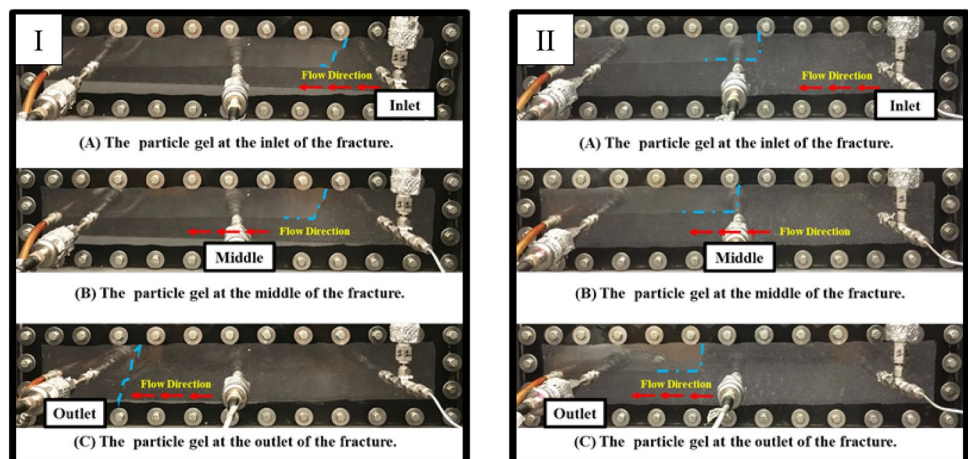
Gel flow with no gravity effect

Figure 3 is divided into two sets of experiment observations, I and II. Set (I) shows the gel particles' movement inside the model for fracture of width 0.5 mm and gel strength of

550 pa. Set (II) shows the gel particles' movement inside the model for the same fracture width but for gel strength of 1450 pa. These two sets of visual results were for the gel size/fracture width ratio larger than one, in which the gel particle size was greater than the fracture width. The gel particles flow was monitored at the fracture inlet (Fig. 3A) through the fracture center (Fig. 3B) and at the fracture outlet (Fig. 3C) using digital camera video. Piston-like gel movement (no signs of gravity effect) across the fracture was observed for the two sets of experiments as it is shown by the colored light blue dot lines. Figure 4 shows the gel transport angle measurements along the fracture length. It is observed that gel flow inside the fracture started with a small angle (40°) at the fracture inlet. However, as the gel transported deep into the fracture, the flow behavior became a piston-like (90°). This result partially agrees with the finding of Zhang and Bai (2010), where they observed that piston-like occurred when the swollen particle sizes were close to the width of the fracture.

Figure 5a shows injection pressure distribution across the fracture for the gel strength of 1450 pa. An increase in pressure was noticed during particle gel movement and stabilized at inlet fracture (46 psi), middle fracture (33

Fig. 3 Gel propagation through fractures: (I) gel particle size to fracture width ratio is 9.76 and (II) particle size to fracture width ratio is 6.4



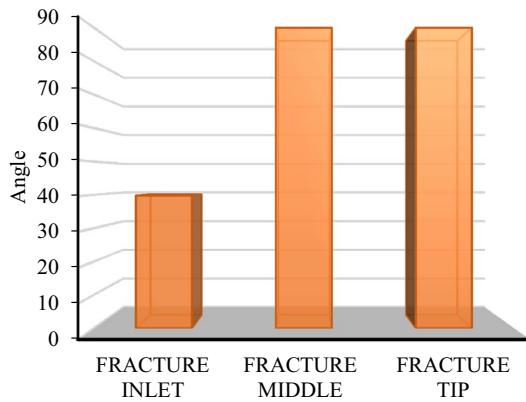


Fig. 4 Gel propagation angles (gel particle size to fracture width ratio is 6.4)

psi), and outlet fracture (28 psi). Interestingly, results in Fig. 5b showed that when the ratio increased from 6.4 to 9.76 (using a gel strength of 550 pa), gel injection pressure decreased instead of increasing. This indicates that not always the gel particle size to the fracture width is the main controller of the passing mechanism but also the gel

strength. The gel strength samples of 550 pa had a larger size than the gel strength samples of 1450, yet it has less injection pressure.

Gel flow with gravity effect

Figure 6I, II shows visual gel propagation performance through fractures. Set I is for gel samples of strength 550 pa transported along a fracture width of 3.2 mm. Set II is for gel samples of strength 550 pa transported along fracture width of 6.75 mm. Similarly, Fig. 7I, II shows visual observations of gel samples of strength 1450 pa transported along a fracture width of 3.2 mm and 6.75 mm, respectively. These four sets of experiments were for the gel size/fracture width ratio equal to or below one, where the gel particle sizes were equal to or smaller than fracture width sizes. All the observations for gel particles move along the fracture as indicated by the colored light blue dot lines showed that the gel propagated with an inclination or steeper inclination performance along the fracture length. As a result, the gel particles were observed to settle down into the fracture due to the gravity effect. Figure 8 shows the gel transport angle measurements along the fracture

Fig. 5 **a** Gel propagation injection pressure through fractures width of 0.5 mm using 1450 pa strength (gel size/fracture width ratio is 6.4) and **b** gel propagation through fractures width of 0.5 mm using 550 pa strength (gel size/fracture width ratio is 9.76)

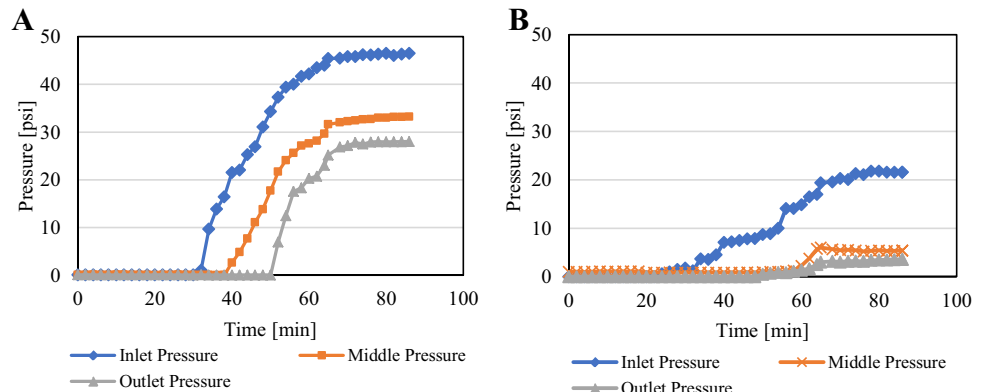


Fig. 6 Gel propagation through fractures: (I) gel particle size to fracture width ratio is 1.5 and (II) gel particle size to fracture width ratio is 0.7

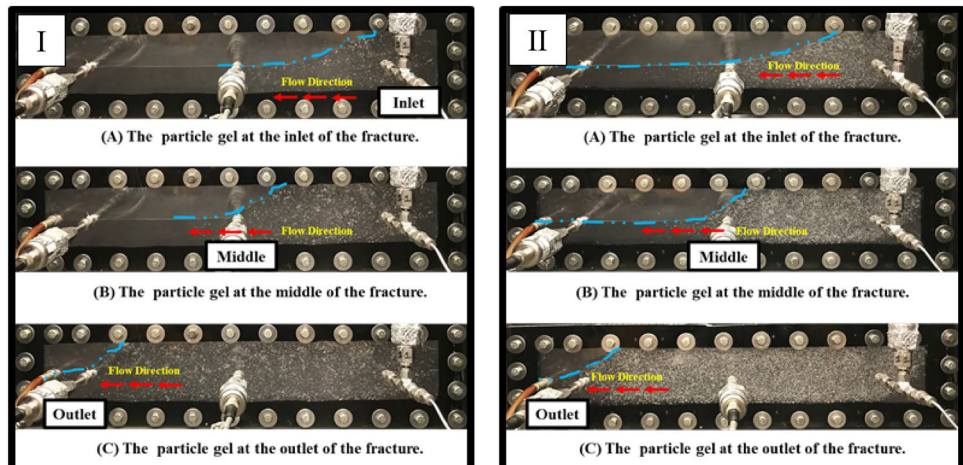


Fig. 7 Gel propagation through fractures: (I) gel particle size to fracture width ratio is 1.0 and (II) gel particle size to fracture width ratio is 0.47

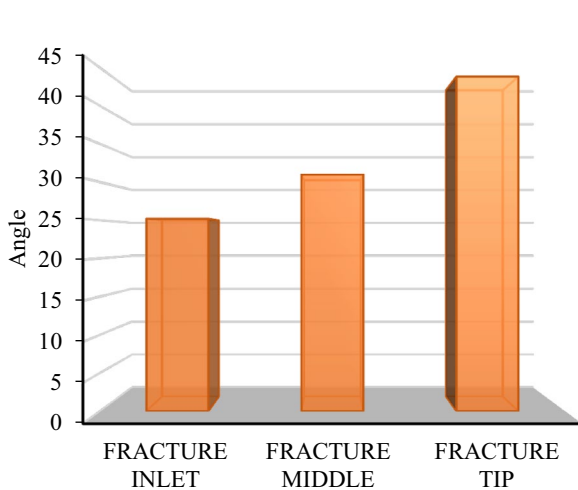
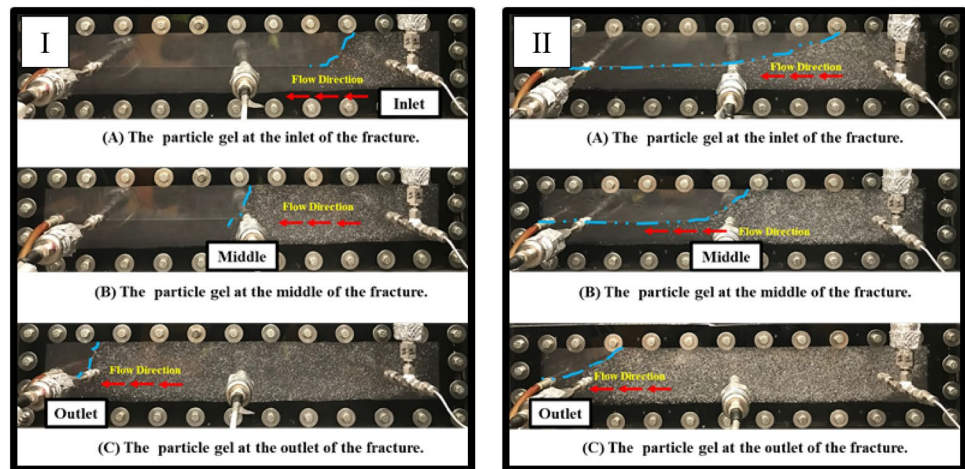


Fig. 8 Gel propagation angles (gel particle size to fracture width ratio is 0.47)

length. At the fracture inlet, gel particles transported with 25° , whereas at the fractured middle the angle became 32° , which is steeper, and finally, at the fracture tip, the angle became 45° . This indicates that as the gel particles move along the fracture, it will begin to develop a steeper angle and thus will not fill the fracture completely, which may affect its ability for water leakage remediation.

Figure 9 shows the pressure change along the fracture until stabilization. Referring to the pressure distribution measurements in Fig. 5a, b, gel injection pressure presented in Fig. 9 was much lower, and this occurred because the gel particle size to fracture width ratio was smaller than 1. The stable pressure was 12.4 psi at the fractured inlet, 8.3 psi at the fractured middle, and 3.8 psi at the fractured outlet. This also shows that as the gel moves further into the fracture, the pressure started to decrease, which is an indication that high gel injection pressure may

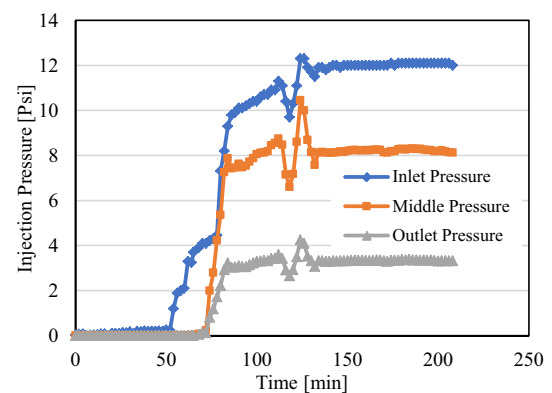


Fig. 9 Gel propagation injection pressure through fractures 6.75 mm using 1450 pa strength (gel particle size to fracture width ratio is 0.47)

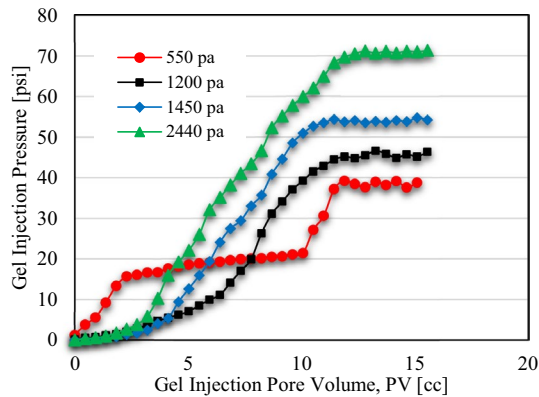
be required for larger and deeper fractures or cracks. Also, since the pressure at the fracture tip was lower compared to the fracture inlet, the gel may have a lower plugging efficiency at the fracture tip compared to the fracture inlet.

Gel particles flow mechanisms

Table 3 gives the summary of gel transport mechanisms of using different gel strengths (550 pa and 1450 pa), two sizes of particle gel (4.88 mm and 3.2 mm), and three fracture widths (0.5 mm, 3.2 mm, and 6.75 mm). The gel movement was piston-like when (D_g/W_f) was much larger than 1. However, gel movement with angle occurred when (D_g/W_f) was close to or smaller than 1. Also, the flow direction changed from inclined to a steeper inclined as the D_g/W_f became smaller than 1. The piston-like angle started with an angle less than 90° at the fracture inlet

Table 3 A summary of the gel particle flow mechanisms across fractures or cracks

| Gel strength [pa] | Particle gel size, Dg [mm] | Fracture width, Wf [mm] | Dg/Wf | Gel flow mechanism | |
|-------------------|----------------------------|-------------------------|-------|--------------------|-----------|
| | | | | Mechanism | Angle [°] |
| 550 | 4.88 | 0.5 | 9.76 | Piston-like | 30–90 |
| | | 3.2 | 1.53 | Inclined | 20–25 |
| | | 6.75 | 0.72 | Steeper inclined | 20–38 |
| 1450 | 3 | 0.5 | 6 | Piston-like | 40–90 |
| | | 3.2 | 0.93 | Inclined | 40–70 |
| | | 6.75 | 0.44 | Steeper inclined | 25–45 |

**Fig. 10** Particle gel injection (0.5 mm fracture width)

and increased to 90° as the gel particle moved deep into the fracture. However, when D_g/W_f was smaller than or equal to 1, the angle started with less than 90° and kept decreasing below 90° as the gel moved deep into fracture due to the gravity effect.

Gel–cement plugging efficiency

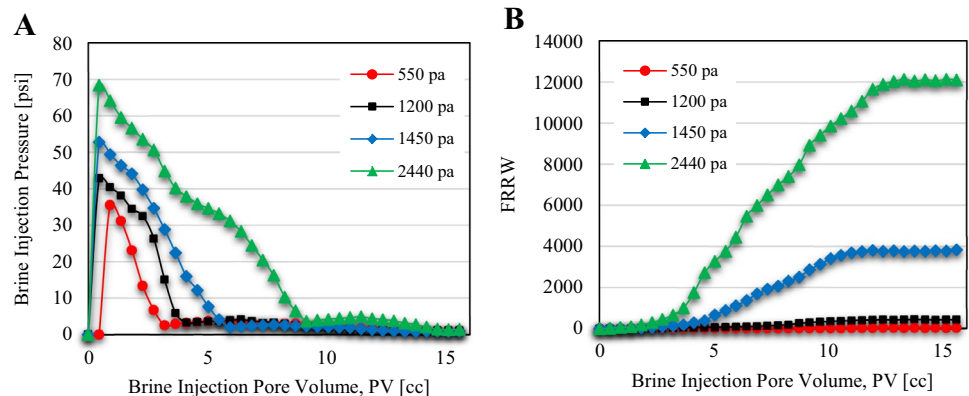
In this section, the ability of the gel to plug cement fractures and control water production was tested using the gel–cement plugging efficiency setup (Fig. 1b).

Effect of gel strength

Figure 10 shows gel injection pressure for different gel strengths. A cement fracture with 0.5 mm was used in this investigation. Gel injection pressure increases as the gel strength increases. The highest gel strength 2440 pa provided the highest pressure value of 70 psi. When the gel strength decreased to 1450, 1200, and 550 pa, the injection stable pressure decreased to 55, 48, and 40 psi, respectively. These results indicate that gel injectivity can be controlled by designing different gel strengths. In referring to the literature, these results show gel particle operation has better injectivity than squeeze cementing jobs. This occurred because gel particles are elastic and deformable materials which allow for this high injectivity compared to solid cement materials.

Resistance to water flow after gel placement

Water breakthrough pressure measurements After gel placement within the cement fracture, brine was injected with constant flow rate to characterize the particle gel blocking behavior against water. Figure 11a shows that the gel with the highest gel strength resulted in the highest pressure to reach a water breakthrough. Gel with 2240 pa strength had the highest water breakthrough pressure at 70 psi, and it decreased to approximately 35 psi when the gel strength

Fig. 11 a Brine injection pressure and b the Frrw (0.5 mm fracture width)

decreased to 550 pa. After the water breakthrough, the pressure decreased until it reached stable pressure. Stronger gel still had higher brine stable pressure compared to gels with lower strengths. The ability of the gel to plug the cement fractures and manage water production is also controllable, and this ability increased by increasing the gel strength.

Water residual resistance factor calculations (*Frrw*) It is defined as the ratio of water phase permeability before and after particle gel treatment. As the *Frrw* value increases, the gel's plugging efficiency increases, and thus a high *Frrw* value is favorable. Equation 2 shows how *Frrw* was calculated in this research:

$$Frrw = \frac{\text{Brine Stable Pressure}_{\text{After Gel}}}{\text{Brine Stable Pressure}_{\text{Before Gel}}} \quad (2)$$

Figure 11b shows that by increasing gel strength, *Frrw* increases. This indicates that increasing gel strength is more effective for water shut-off applications. *Frrw* increased as the gel strength increased; for instance, the *Frrw* of 550 pa gel was 34.5, while the *Frrw* of 2440 pa gel was 12,136. The gel blocking efficiency (*E*) can be represented as the percentage of permeability reduction, which can be calculated from Eq. 3 (Imqam et al. 2015a, b):

$$E (\%) = \left[1 - \left(\frac{1}{Frrw} \right) \right] * 100. \quad (3)$$

The results showed that the plugging efficiency increased when a strong gel was selected as a sealant agent, and *Frrw* ranges from 97 to 99% for all gel strengths. Table 4 lists a summary of gel strength, *Frrw*, and blocking efficiency.

In all experiments, it has been noticed that the brine injection pressure increased sharply until reaching a certain peak, at which point it began to decline. This peak indicates the point at which gel failure and washout began to occur in each section (Seright 2003). After each peak, the pressure declined significantly before becoming stable in all sections. Also, pressure decline was noticed to decline with two humps behavior or single hump behavior based on the gel strength. The hump pressure behavior could occur again if high gel strength was used where more resistance to water flow occurs compared to gels with low strength.

Table 4 A summary of gel strength, *Frrw*, and blocking efficiency

| | | | | |
|-------------------------|------|-------|-------|--------|
| Gel strength [Pa] | 550 | 1200 | 1450 | 2440 |
| <i>Frrw</i> [fraction] | 34.5 | 425 | 3838 | 12,136 |
| Blocking efficiency [%] | 97.1 | 99.77 | 99.97 | 99.99 |

Effect of cement's fracture width

Cement can fail in the annuli of the wellbore for several reasons, and the fractures that are created can have different shapes and sizes. The performance of the gel as a sealant can be affected by the geometry of the fractures. Thus, it is essential to study the effects of the size of the fractures on the sealant before applying any remedial job. In this section, a comparison and analysis are presented to point out the effect of cement fracture width on the gel plugging efficiency. Gel with strength of 1450 pa was used for this investigation. The results of particle gel injection in a fracture of 2 mm width showed a trend similar to that of 0.5 mm width, as shown in Fig. 12. However, increasing the fracture width from (0.5 mm) to (2.0 mm) decreased the gels stabilized pressure from approximately 55 psi to 40 psi, respectively.

Resistance to water flow after gel placement

Water breakthrough pressure measurements The water breakthrough pressure decreased as the fracture width increased at the same injection flow rate, which can be seen in Fig. 13a. The water breakthrough pressure was around 53 psi for the 0.5 mm fracture width and dropped to almost 43 psi for the 2.0 mm fracture width. By increasing the fracture width, the ability of the gel to plug the cement fracture decreased. Figure 13b provides information about the effect of the fracture width on the *Frrw*. The gel strength is 1450 pa, and the fracture widths are 0.5 mm and 2 mm. *Frrw* increased when increasing the fracture width. Table 5 lists the summary of *Frrw* and blocking efficiencies for 1450 pa gel strength. The blocking efficiencies were 97% and 99% for 0.5 mm and 2.0 mm fracture widths, respectively.

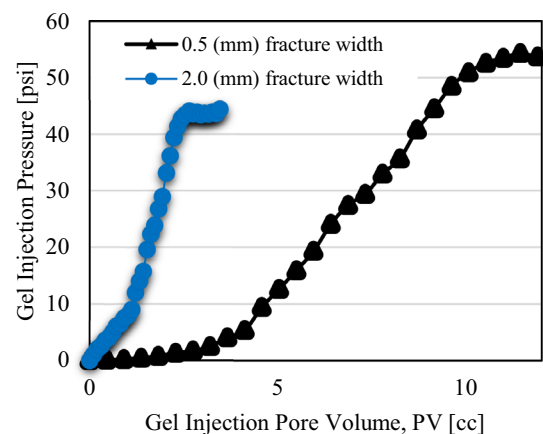


Fig. 12 Particle gel injection in 0.5 mm and 2.0 mm fracture width using 1450 pa gel strength

Fig. 13 **a** Brine injection in 0.5 mm and 2.0 mm fracture width using 1450 pa gel strength and **b** Frrw in 0.5 and 2.0 mm fracture width using 1450 pa gel strength

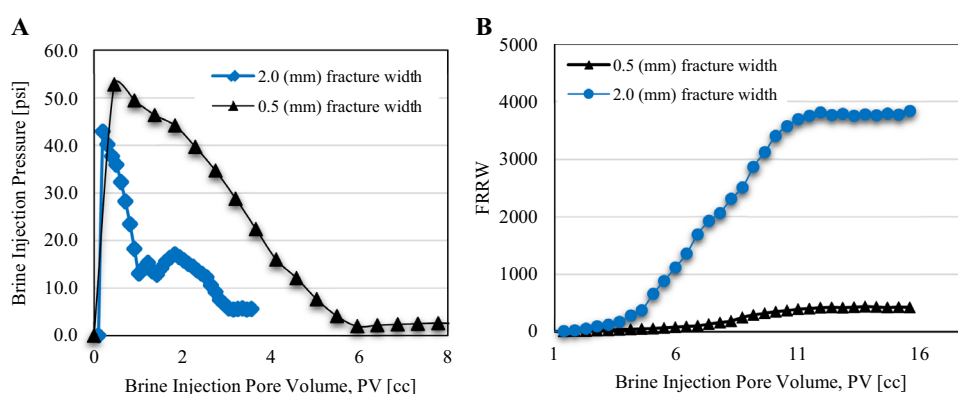


Table 5 Summary of Frrw and blocking efficiency for (1450 pa) gel strength

| | | |
|-------------------------|-----|------|
| Fracture width [mm] | 0.5 | 2 |
| Frrw [fraction] | 425 | 3838 |
| Blocking efficiency [%] | 97 | 99.9 |

Conclusions

By studying the effects of injecting particle gel in cement fractures, several findings were obtained in this study. These findings are based on the analysis of gel swelling capacity measurements, gel strength, gel transportation tests, and gel plugging efficiency experiments. The main conclusions are summarized as follows:

- Polymer gel particles show an acceptable injectivity performance through smaller fractures widths and crack features. However, their plugging performance to water leakage is limited to less than 100 psi. This failure pressure could be controlled by managing the gel strength, but to a certain level.
- The gel particles propagated piston-like when the gel particle size to fracture width ratio was larger than 1. However, it propagates with different angles when the gel particle size to fracture width ratio was equal to or below 1. Thus, it is essential to consider the effect of the cement fracture widths or cracks gaps when gel particles are considered for remedial operations.
- Selecting the gel sealant material not only depends on the plugging efficiency but also on the gel injectivity performance. The gel with high strength had better blocking efficiency but lower injectivity when compared with gel has low strength, and vice versa.

Acknowledgements The author wishes to thank King Abdulaziz University (KAU) for granting him his scholarship.

Open Access This article is distributed under the terms of the Creative Commons Attribution 4.0 International License (<http://creativecommons.org/licenses/by/4.0/>), which permits unrestricted use, distribution, and reproduction in any medium, provided you give appropriate credit to the original author(s) and the source, provide a link to the Creative Commons license, and indicate if changes were made.

References

- Ahdaya M, Imqam A (2019) Investigating geopolymers cement performance in presence of water based drilling fluid. *J Pet Sci Eng*. <https://doi.org/10.1016/j.petrol.2019.02.010>
- Alkhamis M, Imqam A (2018) New cement formulations utilizing graphene nano platelets to improve cement properties and long-term reliability in oil wells. *Soc Pet Eng*. <https://doi.org/10.2118/192342-ms>
- API RP 10B-2 (2012) Recommended practice for testing well cements, 2nd edn. API, Washington, DC
- API Specification 10A/ISO 10426-1 (2010) Specification for cements and materials for well cementing, 23rd edn. API, Washington, DC
- Bai B, Li L, Liu Y, Liu H, Wang Z, You C (2007) Preformed particle gel for conformance control: factors affecting its properties and applications. *Soc Pet Eng*. <https://doi.org/10.2118/89389-pa>
- Cavanagh PH, Johnson CR, Le Roy-Delage S, DeBruijn GG, Cooper I, Guillot DJ, Dargaud B (2007) Self-healing cement—novel technology to achieve leak-free wells. *Soc Pet Eng*. <https://doi.org/10.2118/105781-ms>
- Davies RJ, Almond S, Ward RS, Jackson RB, Adams C, Worrall F, Herringshaw LG, Gluyas JG, Whitehead MA (2014) Oil and gas wells and their integrity: implications for shale and unconventional resource exploitation. *Mar Pet Geol* 56:239–254. <https://doi.org/10.1016/j.marpetgeo.2014.03.001>
- Deng F, Shen X, Liang Q et al (2018) The jamming mechanism of sand control screen for the montmorillonite inflation with the water. *J Pet Explor Prod Technol* 8:189. <https://doi.org/10.1007/s13202-017-0329-z>
- Dusseault MB, Gray MN, Nawrocki PA (2000) Why oilwells leak: cement behavior and long-term consequences. Presented at the SPE international oil and gas conference and exhibition, Beijing, China, 7–10 November. SPE-64733-MS. <http://dx.doi.org/10.2118/64733-MS>
- Feng QH, Chen XC, Sun MD (2012) Study of the multiple-profile control system to enhance oil recovery after polymer flooding. *J Pet Explor Prod Technol* 2:133. <https://doi.org/10.1007/s13202-012-0029-7>

- Fuseni AB, AlSofi AM, AlJulaih AH et al (2018) Development and evaluation of foam-based conformance control for a high-salinity and high-temperature carbonate. *J Pet Explor Prod Technol* 8:1341. <https://doi.org/10.1007/s13202-018-0431-x>
- He H, Wang Y, Sun X et al (2015) Development and evaluation of organic/inorganic combined gel for conformance control in high temperature and high salinity reservoirs. *J Pet Explor Prod Technol* 5:211. <https://doi.org/10.1007/s13202-014-0127-9>
- Imqam A, Bai B, Wei M (2015a) Combining conformance treatment with mobility control improves oil sweep efficiency in non-cross flow heterogeneous reservoirs. *Soc Pet Eng.* <https://doi.org/10.2118/176728-ms>
- Imqam A, Bai B, Al Ramadan M, Wei M, Delshad M, Sepehrnoori K (2015b) Preformed-particle-gel extrusion through open conduits during conformance-control treatments. *Soc Pet Eng.* <https://doi.org/10.2118/169107-pa>
- Imqam A, Bai B, Wei M, Elue H, Muhammed FA (2016) Use of hydrochloric acid to remove filter-cake damage from preformed particle gel during conformance-control treatments. *Soc Pet Eng.* <https://doi.org/10.2118/172352-pa>
- Imqam A, Bai B, Delshad M (2018) Micro-particle gel transport performance through unconsolidated sandstone and its blocking to water flow during conformance control treatments. *Fuel* 231:479–488. <https://doi.org/10.1016/j.fuel.2018.05.099>
- Jones PJ, Karcher J, Ruch A, Beamer A, Smit P, Hines S, Day D (2014) Rigless operation to restore wellbore integrity using synthetic-based resin sealants. *Society of Petroleum Engineers.* <https://doi.org/10.2118/167759-MS>
- Khatri D (2013) Durable cement systems for long term zonal isolation. *DEA technology forum*
- Liu HZ, Zhou M, Wu J et al (2017) Performance evaluation and application of modified urea–formaldehyde resin water shutoff agent. *J Pet Explor Prod Technol* 7:155. <https://doi.org/10.1007/s13202-016-0242-x>
- NORSOK D-010. NORSOK D-010 Rev.4 (2013) Well integrity in drilling and well operations. *Standard Norway, Lysaker*
- Reddy BR, Liang F, Fitzgerald R (2010) Self-healing cements that heal without dependence on fluid contact: a laboratory study. *Society of Petroleum Engineers.* <https://doi.org/10.2118/121555-PA>
- Roth J, Reeves CJ, Johnson CR, DeBruijn GG, Bellabarba M, Le Roy-Delage S, Bulte-Loyer H (2008) Innovative hydraulic isolation material preserves well integrity. *Society of Petroleum Engineers.* <https://doi.org/10.2118/112715-MS>
- Seright RS (1995) Gel placement in fractured systems. *Soc Pet Eng.* <https://doi.org/10.2118/27740-pa>
- Seright RS (2003) Washout of Cr(III)-acetate-HPAM gels from fractures. Paper SPE 80200 presented at the SPE international symposium on oilfield chemistry, Houston, 5–7 February. <https://doi.org/10.2118/80200-ms>
- Seright RS (2009) Disproportionate permeability reduction with pore-filling gels. *Soc Pet Eng.* <https://doi.org/10.2118/99443-pa>
- Tongwa P, Baojun B (2015) A more superior preformed particle gel with potential application for conformance control in mature oilfields. *J Pet Explor Prod Technol* 5:201–210. <https://doi.org/10.1007/s13202-014-0136-8>
- Vasquez J, Santin Y (2015) Organically crosslinked polymer sealant for near-wellbore applications and casing integrity issues: successful wellbore interventions. *Soc Pet Eng.* <https://doi.org/10.2118/175687-ms>
- Watson TL, Bachu S (2007) Evaluation of the potential for gas and CO₂ leakage along wellbores. Presented at the E&P environment and safety conference, Galveston, Texas, 5–7 March. SPE-106817-MS. <http://dx.doi.org/10.2118/106817-MS>
- Yazdani Sadati E, Sahraei E (2019) An experimental investigation on enhancing water flooding performance using oil-in-water emulsions in an Iranian oil reservoir. *J Pet Explor Prod Technol.* <https://doi.org/10.1007/s13202-019-0679-9>
- Yu K, Li K, Li Q et al (2017) A method to calculate reasonable water injection rate for M oilfield. *J Pet Explor Prod Technol* 7:1003. <https://doi.org/10.1007/s13202-017-0356-9>
- Zhang H, Bai B (2010) Preformed particle gel transport through open fractures and its effect on water flow. *Soc Pet Eng.* <https://doi.org/10.2118/129908-ms>
- Zhang M, Bachu S (2011) Review of integrity of existing wells in relation to CO₂ geological storage: what do we know? *Int J Greenhouse Gas Control* 5(4):826–840. <https://doi.org/10.1016/j.ijggc.2010.11.006>
- Zheng LM, Pu CS, Liu J et al (2017) Gel performance in rheology and profile control under low-frequency vibration: coupling application of physical and chemical EOR techniques. *J Pet Explor Prod Technol* 7:479. <https://doi.org/10.1007/s13202-016-0267-1>

Publisher's Note Springer Nature remains neutral with regard to jurisdictional claims in published maps and institutional affiliations.